The Journal of Immunology

Hydrophobic Interactions Are Key To Drive the Association of Tapasin with Peptide Transporter Subunit TAP2

Elke Rufer, Danny Kägebein, Ralf M. Leonhardt and Michael R. Knittler

J Immunol 2015; 195:5482-5494; Prepublished online 30 October 2015;
doi: 10.4049/jimmunol.1500246
http://www.jimmunol.org/content/195/11/5482

The Journal of Immunology is published twice each month by
The American Association of Immunologists, Inc.,
9650 Rockville Pike, Bethesda, MD 20814-3994.

Print ISSN: 0022-1767 Online ISSN: 1550-6606.

Hydrophobic Interactions Are Key To Drive the Association of Tapasin with Peptide Transporter Subunit TAP2

Elke Rufer,* Danny Kägebein,* Ralf M. Leonhardt,[†,‡] and Michael R. Knittler*

The transporter associated with Ag processing (TAP) translocates proteasomally derived cytosolic peptides into the endoplasmic reticulum. TAP is a central component of the peptide-loading complex (PLC), to which tapasin (TPN) recruits MHC class I (MHC I) and accessory chaperones. The PLC functions to facilitate and optimize MHC I–mediated Ag presentation. The heterodimeric peptide transporter consists of two homologous subunits, TAP1 and TAP2, each of which contains an N-terminal domain (N-domain) in addition to a conserved transmembrane (TM) core segment. Each N-domain binds to the TM region of a single TPN molecule, which recruits one MHC I molecule to TAP1 and/or TAP2. Although both N-domains act as TPN-docking sites, various studies suggest a functional asymmetry within the PLC resulting in greater significance of the TAP2/TPN interaction for MHC loading. In this study, we demonstrate that the leucine-rich hydrophobic sequence stretches (with the central leucine residues L20 and L66) in the first and second TM helix of TAP2 form a functional unit acting as a docking site for optimal TPN/MHC I recruitment, whereas three distinct highly conserved arginine and/or aspartate residues inside or flanking these TM helices are dispensable. Moreover, we show that the physical interaction between TAP2 and TPN is disrupted by benzene, a compound known to interfere with hydrophobic interactions, such as those between pairing leucine zippers. No such effects were observed for the TAP1/TAP2 interaction or the complex formation between TPN and MHC I. We propose that TAP/TPN complex formation is driven by hydrophobic interactions via leucine zipper–like motifs. ***The Journal of Immunology*****, 2015, 195: 5482–5494.**

Major histocompatibility complex class I–mediated Ag presentation is a critical immunological pathway to eradicate tumors and virally infected cells (1). To this end, peptide Ags are generated in the cytosol mostly by the proteasome (2). These are then translocated into the endoplasmic reticulum (ER) by the transporter associated with Ag processing (TAP) and loaded onto MHC I molecules in the so-called peptide-loading complex (PLC) (3). The function of the PLC is to facilitate the transfer of peptide Ags, typically 8–11 aa long, into the peptide-binding groove of MHC I and to edit the respective peptide repertoire in a way that only high-affinity ligands are loaded (4). Once MHC I has captured an appropriate peptide ligand, it dissociates from the PLC and migrates via the exocytic pathway to the plasma membrane (5). TAP is a member of the ATP-binding cassette transporter family (4) and forms a heterodimer consisting of two subunits, TAP1 and TAP2. Both TAP subunits have a similar domain structure that can be subdivided into an N-terminal transmembrane domain (TMD), which forms the translocation pore within the ER membrane, and a cytosolic C-terminal nucleotide-binding domain, which energizes peptide translocation (6). The TMDs contain a core domain (core TMD) of six TM α helices and an N-terminal extension of up to four TMs (N-terminal domain [N-domain]) for TAP1 and TAP2, respectively (7). The N-domains in both TAP1 and TAP2 are dispensable for peptide transport, but each contains one single functionally independent docking site for tapasin (TPN) (7). Based on truncation mutants of TAP expressed in insect cells, it had previously been suggested that the first N-terminal TM of each N-domain is crucial for the physical interaction with TPN (8). However, these studies were performed in nonmammalian baculovirus-infected Sf9 cells in the absence of MHC I expression and other accessory PLC polypeptides (8). These accessory proteins normally interact cooperatively with each other as well as with TPN and TAP and substantially stabilize the overall complex (9, 10). Findings by Procko et al. (11) have raised doubts whether the baculovirus/insect cell system employed is in general suitable for the stable expression of intact TAP chains. In fact, the authors found that TAP chains expressed in insect cells are highly sensitive to N-terminal degradation, resulting in a large amount of proteolyzed TAP variants, which are deprived of their N-domain sequences essentially required for TPN binding (11).

In recent years, different groups have confirmed our original finding (3, 7) that the PLC contains two TPN molecules, with one TPN bound to each of the two TAP subunits (12, 13). By analyzing different chimeric TAP/TPN complexes, a current study provides evidence that the nature of TPN recruitment by TAP as a structural basis for proper PLC assembly is highly conserved among jawed vertebrates (14). Most interestingly, we and others also showed that one TPN molecule bound either to TAP1 or TAP2 is sufficient for efficient MHC I Ag presentation (3, 12). However, although both N-domains of TAP contribute independently to MHC I/TPN binding, different studies provided strong evidence for a functional asymmetry resulting in a greater signi-

*Institute of Immunology, Federal Research Institute of Animal Health, Friedrich Loeffler Institute, D-17493 Greifswald–Isle of Riems, Germany; [†]Howard Hughes Medical Institute, New Haven, CT 06519; and [‡]Department of Immunobiology, Yale University School of Medicine, New Haven, CT 06519

Received for publication February 2, 2015. Accepted for publication September 29, 2015.

This work was supported by the Friedrich Loeffler Institute and by Federal Ministry of Education and Research of the Federal Republic of Germany Grant 01 KI 0720. R.M.L. was supported by a fellowship from the Cancer Research Institute.

Address correspondence and reprint requests to Dr. Michael R. Knittler, Institute of Immunology, Federal Research Institute of Animal Health, Friedrich Loeffler Institute, Südufer 10, D-17493 Greifswald-Insel Riems, Germany. E-mail address: michael.knittler@fli.bund.de

The online version of this article contains supplemental material.

Abbreviations used in this article: BN, blue native; ER, endoplasmic reticulum; MHC I, MHC class I; N-domain, N-terminal domain; PLC, peptide-loading complex, TAP, transporter associated with Ag processing; TM, transmembrane; TMD, transmembrane domain; TMLZ, transmembrane leucine zipper motif; TPN, tapasin; wt, wild-type.

www.jimmunol.org/cgi/doi/10.4049/jimmunol.1500246

ficance of the TAP2/TPN interaction for PLC function (7, 15). Consistently, in all avian MHC loci sequenced so far, only TAP2 harbors an N-domain, whereas TAP1 has no such domain and is therefore equivalent to core TAP1 (1ΔN) (16, 17). In our previous studies we demonstrated that a TAP variant lacking the N-domain of TAP1 ("bird-like" TAP variant 1ΔN-2) shows functional recruitment of MHC I and TPN to TAP2 as well as normal MHC I maturation and surface presentation. In contrast, TAP variants lacking the N-domain of TAP2 (1-2ΔN) are disturbed in the proper assembly of the PLC and fail to generate stable MHC I/peptide complexes (7, 18). Thus, 1ΔN-2 with its single TPN-docking site and normal PLC function provides an ideal experimental system to study the TAP2/TPN interaction required for functional MHC I recruitment without any disturbing effects or influence due to TPN binding to TAP1.

In this study, we demonstrate that the first two TMs of TAP2 with their hydrophobic leucine-rich sequence stretches (also known as TM leucine zipper motifs [TMLZ] with the central hydrophobic residues L20 and L66) build a functional unit essential for efficient and functional MHC I/TPN association. In contrast, three highly conserved arginine and aspartate residues located within or directly adjacent to these TMs are not required. Moreover, we demonstrate that the cyclic hydrocarbon benzene known to interfere with the structure and formation of leucine zippers (19, 20) specifically disrupts the physical interaction between TAP and TPN even under stabilizing detergent conditions. Based on our data, we conclude that TM1 and TM2 of TAP2 are essential for the functional interaction with TPN/MHC I. Thus, complex formation between TAP2 and TPN is mainly based on hydrophobic interactions between conserved leucine zipper-like motifs present within the identified TPN docking site of TAP2 and the TM region of TPN.

Materials and Methods

Cell lines and cell culture

T2 is a human TAP-deficient lymphoblastoid cell line expressing HLA-A2 and HLA-B51 (21). T2 cells are derivatives of the TAP-proficient lymphoblastoid cell line T1 (21, 22). Nontransfected T2 and T1 cells were cultured in IMDM/10% FCS (Invitrogen). Transfectants of T2 expressing rat wild-type (wt) TAP (TAPwt), 1ΔN-2, or 1-2ΔN variants (7) were cultured in IMDM (Invitrogen) supplemented with 1 mg/ml G418 (PAA Laboratories). All culture media contained 100 U/ml penicillin and 100 μg/ml streptomycin (Invitrogen).

Benzene-PLC stability assay

Cells were lysed in digitonin-containing lysis buffer with or without benzene (0.05–5%) for 30 min at room temperature. Benzene does not affect the cholesterol-binding properties of digitonin (23). For immunoisolation, postnuclear cell extracts were applied for 24 h at 4°C to Sepharose coupled anti-TAP2 Abs. After extensive washing with lysis buffer, precipitated proteins were eluted in 100 mM Tris/0.5% SDS (pH 9.0), separated by SDS-PAGE, and analyzed in Western bots. Benzene is a carcinogen (http://www.cancer.org/cancer/cancercauses/othercarcinogens/intheworkplace/benzene) and extreme care should be exercised in its use.

Cloning and expression of truncated and mutant TAP chains

The vector pBluescript II KS$^+$ (Stratagene) containing rat TAP2a cDNA (http://www.ncbi.nlm.nih.gov/genbank/, GenBank accession number X63854.1) was subjected to QuikChange site-directed mutagenesis (Stratagene) using primer pairs 5′-GCAGCCGCAGACCCCACCATGGCGCCCGGCACCCTGCGACTTGGAGTG-3′ and 5′-CACTCCAAGTCGCAGGGTGCCGGGCGCCATGGTGGGGTCTGCGGCTGC-3′, 5′-GCAGCCGCAGACCCCACCATGGCGCCCACCATGAGCACCTCAG-3′ and 5′-CTGAGGTGCTCATGGTGGGCGCCATGGTGGGGTCTGCGGCTGC-3′, 5′-CCATGGCGCTGTCCTACCCGGCGCCCTGGGCTAGCCTGCTGCTGGTGGACCTGGC-3′ and 5′-GCCAGGTCCACCAGCAGCAGGCTAGCCCAGGGCGCCGGGTAGGACAGCGCCATGG-3′, 5′-GGGCCTCTCTGCTGCTGGTAGCGCTGGCTTTACTTGGGTTGCTACAAAG C-3′ and 5′-GCTTTGTAGCAACCCAAGTAAAGCCAGCGCTACCAGCAGCAGAGAGGCCC-3′, 5′-GGGCCTCTCTGCTGCTGGTGAGGCTAGCTTTACTTGGGTTGCTACAAAGC-3′ and 3′-GCTTTGTAGCAACCCAAGTAAAGCTAGCCTCACCAGCAGCAGAGAGGCCC-5′, 5′-CCCCCTGTTTTTCTCGCTGGCAGCACTAGTGGGAAGCACCATGAGCACC-3′ and 5′-GGTGCTCATGGTGCTTCCCACTAGTGCTGCCAGCGAGAAAAACAGGGGG-3′, and 5′-CCCCCTGTTTTTCTCGCTGGACGCACTAGTGGGAAGCACCATGAGCACC-3′ and 5′-GGTGCTCATGGTGCTTCCCACTAGTGCGTCCAGCGAGAAAAACAGGGGG-3′ to generate the 1ΔN-2 variants 1ΔN-2ΔTM1 (39 deleted residues downstream of sequence position 2), 1ΔN-2ΔTM1/2 (83 deleted residues downstream of sequence position 2), and 1ΔN-2R/A-7, 1ΔN-2D/A-16, 1ΔN-2D/R-16, 1ΔN-2R/A-80, and 1ΔN-2R/D-80, respectively, before cloning into pHβApr1neo (24). To generate the TAP2 mutants TAP2 L/A-20, TAP2 L/A-66, and TAP2 L/A-20:66, the cDNA of rat TAP2a (http://www.ncbi.nlm.nih.gov/genbank/; GenBank accession no. X63854.1) was subjected to QuikChange site-directed mutagenesis using primer pairs 5′-CTGCTGCTGGTGGAGCTAGCTTTAGCTGGGTTGCTACAAAGCTCTCTGGG-3′ and 5′-CCCAGAGAGCTTTGTAGCAACCCAGCTAAAGCTAGCTCCACCAGCAGCAG-3′ and 5′-GGGCTGCTGAGACTCGTGGGTACCTTTGCGCCCTTGCTCTGCCTGACTAACCCC-3′ and 5′-GGGGTTAGTCAGGCAGAGCAAGGGCGCAAAGGTACCCACGAGTCTCAGCAGCCC-3′. All TAP constructs were fully sequenced and transfected into T2 cells by using the Nucleofector II device from Lonza. For transient transfection of T2 cells with TAP2, TAP2 L/A-20, TAP2 L/A-66, and TAP2 L/A-20:66 constructs were cloned into pcDNA3 (Invitrogen). T2 cells were then cotransfected via nucleofection (Lonza) by using the four different TAP2 constructs. Twenty-four hours after nucleofection, the transfectants were analyzed by fluorescent microscopy (Nikon Eclipse T1100/CoolLED PE200) (the transient transfection efficiency reached values up to 65%).

Antibodies

116/5 and D90 are rabbit antisera recognizing the C terminus of rat TAP2 or rat TAP1 (25, 26). MAC394 is a monoclonal mouse anti-rat TAP2 Ab derived from immunization with the recombinant histidine-tagged cytoplasmic domain of rat TAP2a (27). The mouse mAbs 148.3 and 435.3 are directed against human TAP1 and TAP2, respectively (28, 29). 3B10.7 is a rat mAb binding the H chains of HLA-A and HLA-B. 4E is a β_2-microglobulin□dependent mouse mAb that recognizes an epitope common to all assembled HLA-B molecules (30). The rabbit antiserum R.SinE and the mouse mAb PasTa-1 are raised against human TPN (31). All HRP-conjugated Abs were purchased from Dianova.

Cell lysis, endoglycosidase H digest, and Western blotting

Equal number of cells were lysed in PBS containing 1% digitonin (Sigma) or 1% Triton X-100 (Sigma). Endoglycosidase H digest of cell extracts was performed as described earlier (7). Cell lysates were separated by SDS-PAGE and analyzed by Western blotting. Fluorographs were scanned and quantitated using the software GelEval from FrogDance.

Immunoprecipitation

Abs (anti–rat TAP2/MAC394, anti-hTAP2/435.3, and anti-TPN/PasTa-1) used for immunoprecipitation were coupled to cyanogen bromide–activated Sepharose (Sigma-Aldrich). For immunoisolation experiments cells were washed in PBS before lysis in 1% digitonin (Sigma-Aldrich). Postnuclear supernatants were applied for 2 h at 4°C to the Sepharose-coupled Abs. After extensive washing with 0.1% digitonin, precipitated proteins were eluted in 100 mM Tris/0.5% SDS (pH 9.0). Eluted samples were separated by SDS-PAGE and analyzed in Western bots.

Pulse-chase analysis

The pulse-chase analysis was carried out as described previously (7).

Blue native–PAGE analysis

Blue native (BN)–PAGE analysis was carried out as described by Schägger et al. (32) with the following modifications. Cells (10^6) were lysed in 100 μl BN buffer (25 mM Bis-Tris–HCl [Sigma-Aldrich], pH 7, 20% glycerol) containing 1% digitonin (Sigma-Aldrich). Lysates were separated by BN-PAGE (gel gradient, 5.0–13.5% polyacrylamide) at 4°C. Before sample loading, 20 μl lysates was mixed with 2 μl BN sample buffer (100 mM Bis-Tris–HCl [Sigma-Aldrich], 0.5 M 6-aminocaproic acid [Sigma-Aldrich], pH 7.0, 30% sucrose, 50 mg Serva G (Serva) and incubated for 10 min on ice. As protein markers we used aldolase (158 kDa), the 24-mer (440 kDa) and the 48-mer form (880 kDa) of ferritin. BN gels were run for 5–6 h. The gel run was performed with cathode (50 mM Tricine,

15 mM Bis-Tris [pH 7.0], 0.01% Serva G) and anode buffers (25 mM Bis-Tris [pH 7.0]). The blue cathode buffer was exchanged with a colorless cathode buffer during the run after 6–8 h. For immunoblotting, the BN gel was incubated for 10 min in transfer buffer (25 mM Tris, 192 mM glycine, 20% methanol) containing 0.1% SDS. Immunoblots were developed with specific Abs against rat TAP1, rat TAP2, TPN, and MHC I H chains.

Flow cytometry

Flow cytometry was performed on a FACSCalibur (BD Biosciences) as described previously (33). For the analysis cells were stained with mAb 4E followed by FITC-labeled secondary Ab.

Peptide transport assay

The nonradioactive peptide transport assay using the model peptide S8 (TVDNKTRYR, which is biotin labeled at the lysine residue) was carried out as described by Keusekotten et al. (34).

Results

The first two leucine-rich TM segments of TAP2 are involved in functional TPN/MHC I recruitment

Previously, we had shown that the TAP variant 1ΔN-2 (Fig. 1A) forms a stable and fully functional PLC with only one TPN-docking site provided by TAP2 (7). This mimics the situation in the avian system, in which only TAP2 but not TAP1 contains an N-domain (16). Thus, our bird-like TAP variant 1ΔN-2 provides an excellent starting point to study the function of the N-domain in TAP2 without potential interference from TPN binding to TAP1. To this end, we assessed which TMs of TAP2 are involved in the functional interaction with TPN/MHC I.

Each of the first two N-terminal TMs (TM1 and TM2, predicted by TopPred II; see Fig. 1B) (35), but not the third TM (TM3, not shown) of TAP2 contains leucine-rich sequence stretches, so-called TMLZs (36). The same is also true for TM1 and TM2 of TAP1 (Fig. 1C). These motifs were speculated to serve as complementary interaction sites for a possible leucine zipper in the single TM segment of TPN (Fig. 1D) (37). Consistent with such a role, the putative TMLZs in all these TMs are well conserved (Fig. 1B–D). Moreover, a comparison of helical wheel projections of TM1 from TAP1 and TAP2 indicates a similar spatial topology of hydrophobic and polar surface residues/areas (Fig. 1B, 1C, *right panel*). A comparable situation can be also seen for the helical wheel projections of TM2 from TAP1 and TAP2 (Fig. 1B, 1C, *right panel*).

T2 cells expressing 1ΔN-2 variants bearing single and/or multiple mutations within the TMLZs of TM1 and TM2 in TAP2 could not be established (not shown). This suggests that stable expression of the respective mutant transporters is either harmful to the transfectants or that the transporter is structurally unstable and rapidly degraded. Thus, based on the original TAP variant 1ΔN-2 (Fig. 1A) (7), we generated transporters lacking the entire TM1 or lacking both TM1 and TM2 of TAP2 (1ΔN-2ΔTM1 and 1ΔN-2ΔTM1/2, Fig. 1A). Both TAP variants were expressed at levels comparable to TAPwt and showed normal peptide transport activity (Fig. 2A, 2B). To investigate whether the mutant transporters interact with TPN and MHC I, we performed immunoisolations of TAP and/or TPN from digitonin-lysed cells (Fig. 2C). This revealed that the transporter variant 1ΔN-2ΔTM1 retains the ability to interact with TPN and MHC I to a significant extent (~50–60% reduced co-isolation). Only in the case of 1ΔN-2ΔTM1/2 was the formation of the PLC completely disrupted (Fig. 2C). The distinct behavior of TAPwt, 1ΔN-2ΔTM1, and 1ΔN-2ΔTM1/2 was also reflected in different intracellular MHC I maturation profiles, as well as in differences in assembly-dependent thermostability and surface expression of MHC I (Fig. 2D–G). T2 transfectants expressing 1ΔN-2ΔTM1 displayed an increased amount of ER-localized and thermolabile MHC I molecules. This was accompanied by a reduction in surface levels of HLA-B5, an MHC I allele known for its TPN-dependent peptide loading and maturation (38). Strikingly, all these phenotypic deficiencies were significantly more pronounced in T2 transfectants expressing TAP variant 1ΔN-2ΔTM1/2. BN gel electrophoresis assays (Fig. 3) confirmed our previous finding that TAPwt forms oligomers of 350 and 450 kDa (3), whereas 1ΔN-2 participates in 230- and 330-kDa complexes (3). Interestingly, the analysis of variant 1ΔN-2ΔTM1 revealed that a large fraction (~30–40%) of this TAP variant did not interact with TPN (presence of an additional 130-kDa complex) (Fig. 3B). Furthermore, in the case of 1ΔN-2ΔTM1/2, only a TPN-free transporter species of ~130 kDa was present (Fig. 3B). This demonstrates that the physical recruitment of TPN is weakened for 1ΔN-2ΔTM1 and completely disrupted for 1ΔN-2ΔTM1/2. Thus, our results indicate that the first two N-terminal TMs of TAP2 with their highly conserved leucine-rich sequence stretches act together to form a functional unit required for efficient binding of TPN and MHC I.

Highly conserved charged residues within and/or adjacent to the first two TMs of TAP2 are dispensable for TPN/MHC I binding

Salt bridges in assembled TM helices are formed by the complementary combinations D-R, D-K, E-R, and E-K (39). Glutamate, lysine, and arginine are thought to be suited for a dual role forming ionic as well as hydrophobic interactions, whereas the side chain of aspartate is obviously too short to contribute significantly to hydrophobic interactions (40, 41). Mutations of a highly conserved glutamate flanking the TPN TM on the ER luminal side affect TAP2 stabilization as well as complex formation (37). However, it is not clear whether this conserved acidic residue is required for proper TPN folding, TAP interaction, or the complex formation with other accessory components of the PLC, such as the ER-resident chaperone calnexin (42).

To get more insight into this, we concentrated our studies on the six highly conserved charged residues within or adjacent to the leucine-rich regions of TM1 and TM2 at positions 7 (arginine), 16 (aspartate), 41 (glutamate), 45 (arginine), 54 (lysine), and 80 (arginine) and asked whether these amino acids play a role in the TAP2/TPN interaction. Alanine substitutions at positions 7, 16, and 80 seem to have no detrimental effects on the expression level and stability of 1ΔN-2 (Fig. 4A), and this was also true for charge-exchange mutations at position 16 and 80 (D to R and R to D, respectively). Only some minor degradation (10–20%) could be observed for the transporter mutant 1ΔN-2R/A-80 (Fig. 4A, indicated by an asterisk). In contrast, the conserved residues glutamate, arginine, and lysine at positions 41, 45, and 54 in the loop connecting TM1 and TM2 did not tolerate any of these amino acid alterations without affecting cellular synthesis and/or stability of the transporter (not shown). Thus, we focused on the five expressible TAP mutants (1ΔN-2R/A-7, 1ΔN-2D/A-16, 1ΔN-2D/R-16, 1ΔN-2R/A-80, and 1ΔN-2R/D-80). All these transporters were expressed at levels comparable to 1ΔN-2 or TAPwt (Fig. 4A, *left panel*) and displayed efficient subunit dimerization (Fig. 4A, *right panel*) and normal peptide transport activity (Fig. 4B). Analysis of immunoisolated TAP or TPN complexes showed that none of the mutant TAPs was detectably impaired in complex formation with TPN and MHC I (Fig. 4C). Intracellular maturation, stability, and surface expression of MHC I were normal (Fig. 4D–F), indicating that the respective PLCs are functional. All mutant transporters promoted MHC I surface presentation to a comparable extent as TAPwt and 1ΔN-2 (Fig. 4G). This suggests that the acidic and

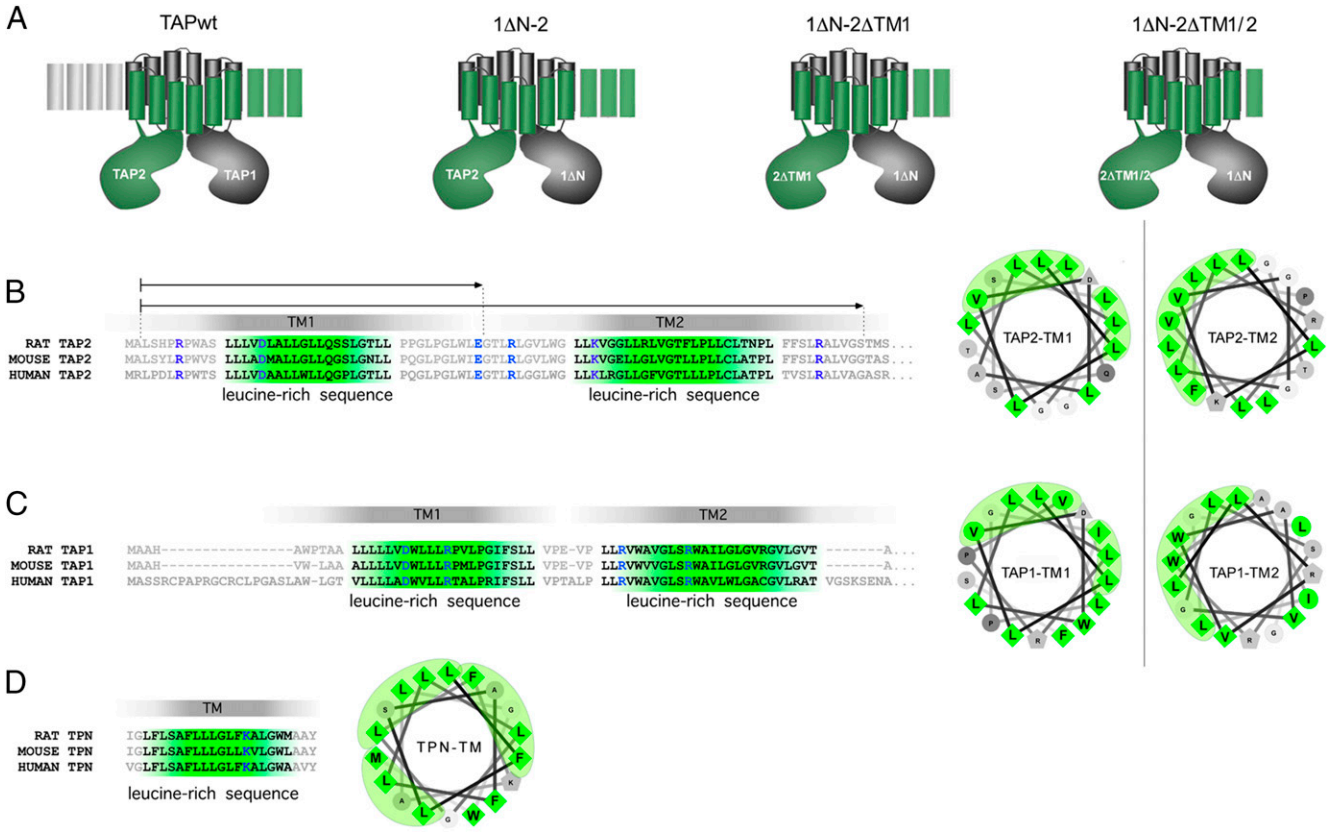

FIGURE 1. Schematic diagrams of TAP variants and sequence properties of the first two TM regions of TAP1, TAP2, and the TM region of TPN. (**A**) Schematic diagrams of TAPwt and the transporter variants 1ΔN-2, 1ΔN-2ΔTM1, and 1ΔN-2ΔTM1/2. (**B**) Sequence alignment (rat, mouse, human, *left*) and helical wheel projections of the TM1 and TM2 α helix of TAP2 (rat, *right*). Sequence alignments were accomplished with the program CLC Sequence Viewer. Topology prediction of the TMDs was performed with TopPred II. Helical wheels were generated using the online tool "helical wheel projection" created by Don Armstrong and Raphael Zidovetzki (version ID: wheel.pl,v 1.4 2009-10-20 21:23:36 don Exp). The highly conserved leucine-rich regions and the hydrophobic residues/patches in the helical wheel projection of TM1 and TM2 are shown in green. Conserved charged residues are indicated by blue letters. Arrows mark the N-terminal regions that were truncated to generate the deletion TAP2 variants 2ΔTM1 and 2ΔTM1/2 lacking 39 and 83 residues, respectively, downstream of sequence position 2. (**C**) Sequence alignment (rat, mouse, human, *left*) and helical wheel projections of the predicted TAP1 TM segments TM1 and TM2 (rat, *right*). (**D**) Sequence alignment (rat, mouse, human, *left*) and helical wheel projection of the predicted TM segment of TPN (rat, *right*). All sequences were retrieved from the GenBank database (http://www.ncbi.nlm.nih.gov/genbank/) (GenBank accession nos. AJ400732.1, AJ316613.2, AF009510.1, X63854.1, NM_011530.3, AB073779.1, X57523.1, NM_001161730.1, and AY523971.2).

basic characters of the three highly conserved charged residues within or directly adjacent to TM1 and TM2 are not only negligible for TAP expression, stability, and peptide transport but are also dispensable for the functional recruitment of TPN and MHC I.

The TAP/TPN interaction in the PLC is sensitive to leucine zipper–targeting aromatic hydrocarbons

Previously, it had been shown that TAP and TPN form a stable complex that does not disassemble after the release of loaded MHC I from the PLC (Fig. 5A) (43). Our findings in Fig. 4 do not exclude the possibility that acidic or basic residues, which were not mutable in TAP2 (E41, R45, and K54), are involved in the assembly of TAP and TPN. However, note that the TAP/TPN interaction is also stable in cell extracts in the presence of the sterol-binding mild detergent digitonin that does not physically disrupt hydrophobic or other biochemical interactions within protein complexes. In contrast, Triton X-100, which abrogates hydrophobic interactions but maintains charge–charge and hydrogen bonding between polypeptides, releases TPN from TAP (Fig. 5B) (44). Hence, to get more insight into the biochemical properties of the TAP/TPN interaction, we performed stability assays (Fig. 5C) using the cyclic hydrocarbon benzene. Benzene binds efficiently to cellular membranes (45), interacts with hydrophobic protein patches and/or cores, and modulates the arrangement of hydrophobic protein interfaces (19, 20). Benzene does not affect the cholesterol-binding properties of digitonin (23), but it specifically targets leucine zippers containing central small residues (19, 20) (see Fig. 1). Leucine zippers are made up of two or more packed α helices (containing 20–40 residues) (46), with every seventh residue containing leucine or some other large hydrophobic residue, such as isoleucine, valine, methionine, or phenylalanine (47). Also, conserved tryptophan and glycine residues are thought to play a role in hydrophobic helix–helix packing (48). The leucine zipper–like sequence stretches of TM1 and TM2 in TAP2 and TAP1 contain such characteristic hydrophobic amino acids (Fig. 1). When analyzing digitonin-solubilized T2-TAPwt cells we observed that TPN dissociation from TAP is triggered in vitro by benzene in a concentration-dependent manner. At a concentration of 5% benzene, nearly all of the TPN molecules were released from TAP (Fig. 5C). No such effects were observed with other cyclic hydrocarbons (e.g., dioxane alone), which specifically disrupt hydrophobic lipid/lipid and lipid/protein interactions in biological membranes (not shown) (49, 50). Moreover, although benzene has apparently no detectable effect on the proper transport function of TAP (Fig. 5D), surface MHC I was detectably thermolabile in the presence of benzene (Fig. 5E, *left* and *right panels*), suggesting the

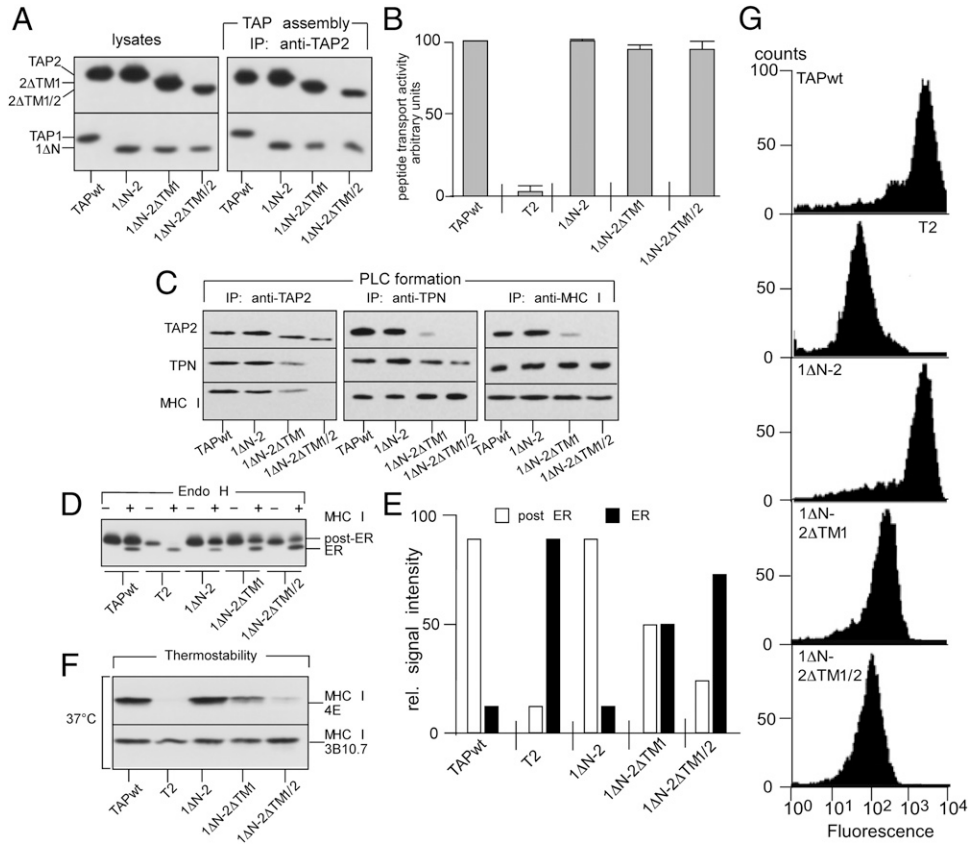

FIGURE 2. First and second TM regions (TM1 and TM2) of TAP2 are essential for efficient TPN/MHC I binding. (**A**) TAP chain assembly. T2 transfectants expressing the TAPwt or the TAP variants 1ΔN-2, 1ΔN-2ΔTM1, and 1ΔN-2ΔTM1/2 were lysed in digitonin containing lysis buffer and subjected to immunoprecipitation using the anti-TAP2 antiserum 116.5. Lysate controls and immunoprecipitates were analyzed in Western blots probed for TAP1 and TAP2. (**B**) Transport activity of wt and truncated TAP variants was measured by a colorimetric assay as described in *Materials and Methods*. The bar graphs represent the average values of experiments carried out in duplicate. (**C**) T2 transfectants were lysed in digitonin, immunoprecipitated with anti-TAP2 (*lanes 1–4*), anti-TPN (*lanes 5–8*), or anti–MHC I (*lanes 9–12*), and analyzed by Western blotting. (**D** and **E**) Intracellular maturation of MHC I was assessed by incubating cell lysates with endoglycosidase H (Endo H) followed by Western blotting using the mAb 3B10.7. Signal quantification was performed by densitometry. (**F**) Cell lysates of the T2 transfectants were incubated for 1 h at 32°C. The thermostability of HLA-B5 was analyzed by immunoprecipitation using the conformation-dependent and -independent mAbs 4E and 3B10.7. Precipitates were analyzed by Western blotting using mAb 3B10.7. (**G**) Cells were incubated with mAb 4E followed by FITC-labeled secondary Ab. Surface expression of MHC I was determined by flow cytometry. Histograms show life-gated cells.

presentation of an altered peptide repertoire. In view of the fact that TPN recruitment to the PLC is essential for a proper quality control of MHC I peptide loading (7, 51), it is tempting to assume that the result of the experiment depicted in Fig. 5E reflects a loss of this critical MHC I control step. Next, we asked whether other TAP variants and further polypeptide interactions within the PLC are affected by hydrocarbon treatment. Therefore, T2 cells expressing TAPwt, 1-2ΔN (TAP lacking the TPN docking site in TAP2), 1ΔN-2 (TAP lacking the TPN docking site in TAP1) (7), and T1 cells (expressing human endogenous TAP) (21) were lysed in digitonin lysis buffer in the presence or absence of benzene (Fig. 6). Western blot analysis of immunoisolated PLCs demonstrated a benzene-dependent disruption of the TAP/TPN interaction for all analyzed TAP complexes (Fig. 6A, 6B). TAP/TPN interactions in T1 cells and T2 transfectants displayed comparable benzene susceptibility (Fig. 6C, 6D), suggesting similar hydrophobic requirements for complex formation. In contrast, complex formation between TAP1 and TAP2 or between TPN and MHC I was not affected at all by the presence of the hydrocarbon (Fig. 6). Because we used different Abs to study TAP2/TAP1, TAP/TPN, and TPN/MHC I interactions, we additionally analyzed different protein loads (24, 12, 6, and 3 μl) of the various immunoisolates to validate the differential effects of benzene on the PLC components (Supplemental Fig. 1). As expected, at comparable signal intensities of immunoisolated TAP chains the amount of co-isolated TPN was drastically reduced in the presence of benzene (Supplemental Fig. 1). A comparable situation was also found for precipitated TPN and co-isolated TAP2. Again, the different sample loads confirmed a benzene-mediated dissociation of TPN/TAP complexes. In contrast, a comparison of the obtained signal ratios for immunoisolated TAP2 and co-isolated TAP1 demonstrated their stable complex formation in the presence of benzene (Supplemental Fig. 1). This was also true for the obtained MHCI/TPN signal ratios of the anti-TPN precipitates and thus confirmed that TPN and MHC I form a benzene-resistant complex.

Taken together, our results indicate that the biochemical nature of physical TPN interaction with assembled TAP molecules is comparable for TAP1 and TAP2 and predominantly determined by benzene-sensitive hydrophobic interactions.

The three TPN-docking sites in TAP have distinct biochemical requirements for TPN binding

Single as well as assembled TAP2 chains interact with TPN exclusively via the N-domain (7), whereas single TAP1 subunits use a TPN-docking site in the core TMD (7, 52), which is lost upon TAP2 association (52). The respective TPN-binding site of core

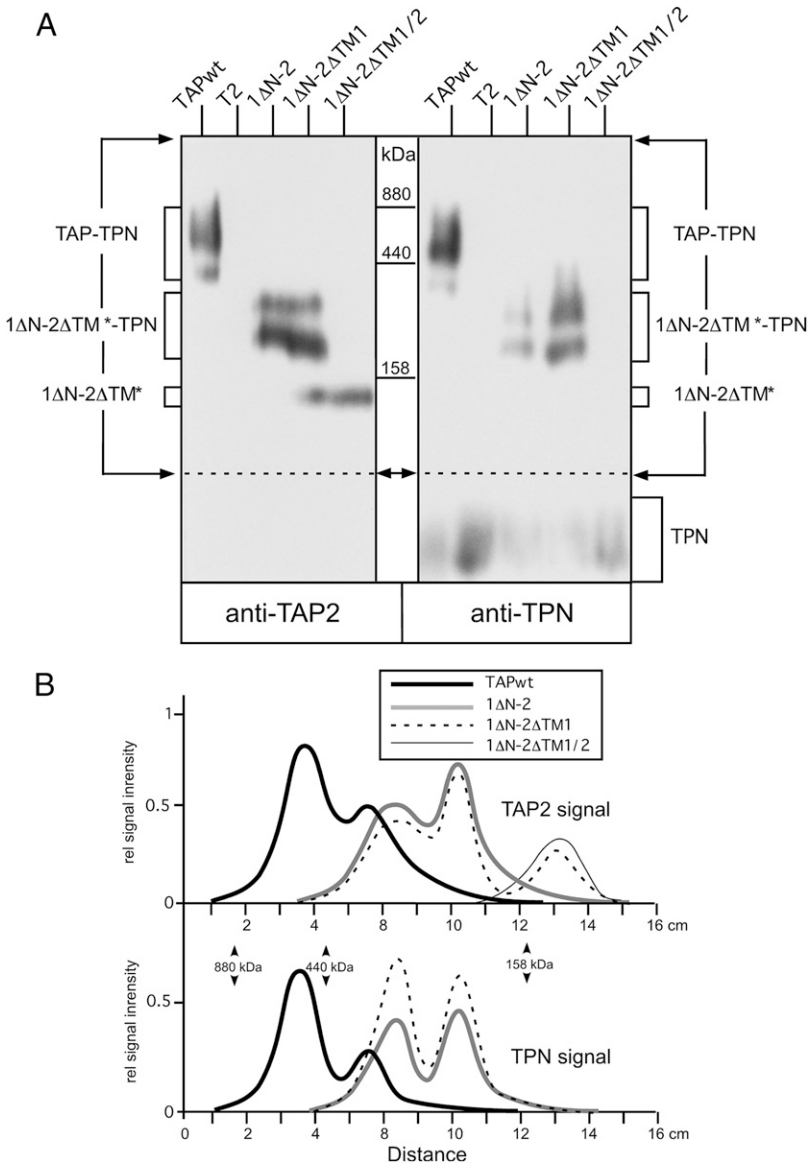

FIGURE 3. Electrophoretic migration of native PLCs formed by TAPwt and truncated TAP variants. (**A**) T2 transfectants were lysed in stabilizing BN buffer containing 1% digitonin. Cell lysates were separated by BN-PAGE and analyzed by Western blotting. The Western blot signals of variants 1ΔN-2ΔTM1 and 1ΔN-2ΔTM1/2 are indicated by 1ΔN-2ΔTM*. (**B**) For signal quantification of the immunoblots, the different tracks were scanned in a linear mode by densitometry. Arrows and dotted lines indicate the scanning area in the Western blots (A).

TAP1 is located in the polar face of the amphipathic TM9 and depends on charged and polar but not hydrophobic residues (52). Thus, the biochemical nature of the long-lasting, structural interaction between TPN and the TAP N-domains, driven by hydrophobic leucine zippers, appears to be strikingly different from the transient, polar interaction between TPN and the core TMD of TAP1. Therefore, a surprising scenario emerges in which TAP and TPN may have two radically different modes of interaction, although both are acting via TM segments and in the case of TPN even involve the same single TM segment. To address such a scenario directly, we analyzed how the physical interaction of TPN with unassembled TAP1 and TAP2 subunits differs with respect to benzene sensitivity. To this end, a series of different sample volumes (24, 12, 6, and 3 μl) of anti-TAP1 and anti-TAP2 immunoprecipitates was analyzed by Western blotting using Abs against TAP1, TAP2, and TPN. As shown in Fig. 7, only TAP2/TPN complexes were highly sensitive to benzene, whereas TAP1/TPN and 1ΔN/TPN complexes were not affected by the cyclic hydrocarbon (see TPN/TAP chain signal ratios for the different protein loads). Thus, consistent with a recent study (52), the transient complex formation between TPN and the core TMD of single TAP1 chains does not appear to be driven by hydrophobic interactions. We note that these results are also an excellent internal control for all of our above experiments, as they demonstrate that benzene selectively disrupts only hydrophobic interactions, even among identical binding partners (i.e., TPN binding to the N-domain of TAP1 is fully benzene sensitive; Fig. 6, S1, T2-TAPwt, and T1 cells), whereas binding to the core TMD of TAP1 is completely benzene insensitive (Fig. 7, T2-1ΔN). Taken together, our data strongly support an exciting scenario in which the TPN-docking sites in the N-domain of TAP2 and in the core TMD of TAP1 indeed display strikingly different biochemical requirements, likely correlating with different functions of the respective interactions.

Mutations of leucine residues within the TMLZ of single TAP2 chains weaken the physical interaction with TPN

As mentioned above, stable T2 transfectants expressing 1ΔN-2 variants carrying TMLZ mutations in TM1 and/or TM2 cannot be established. However, three TAP2 single-chain mutants (TAP2 L/A-20, TAP2 L/A-66, and TAP2 L/A-20:66) showed measurable expression when transiently transfected into T2 cells (Fig. 8A). As expected, all of them colocalized well with TPN in the ER (Supplemental Fig. 2). To analyze the physical complex formation

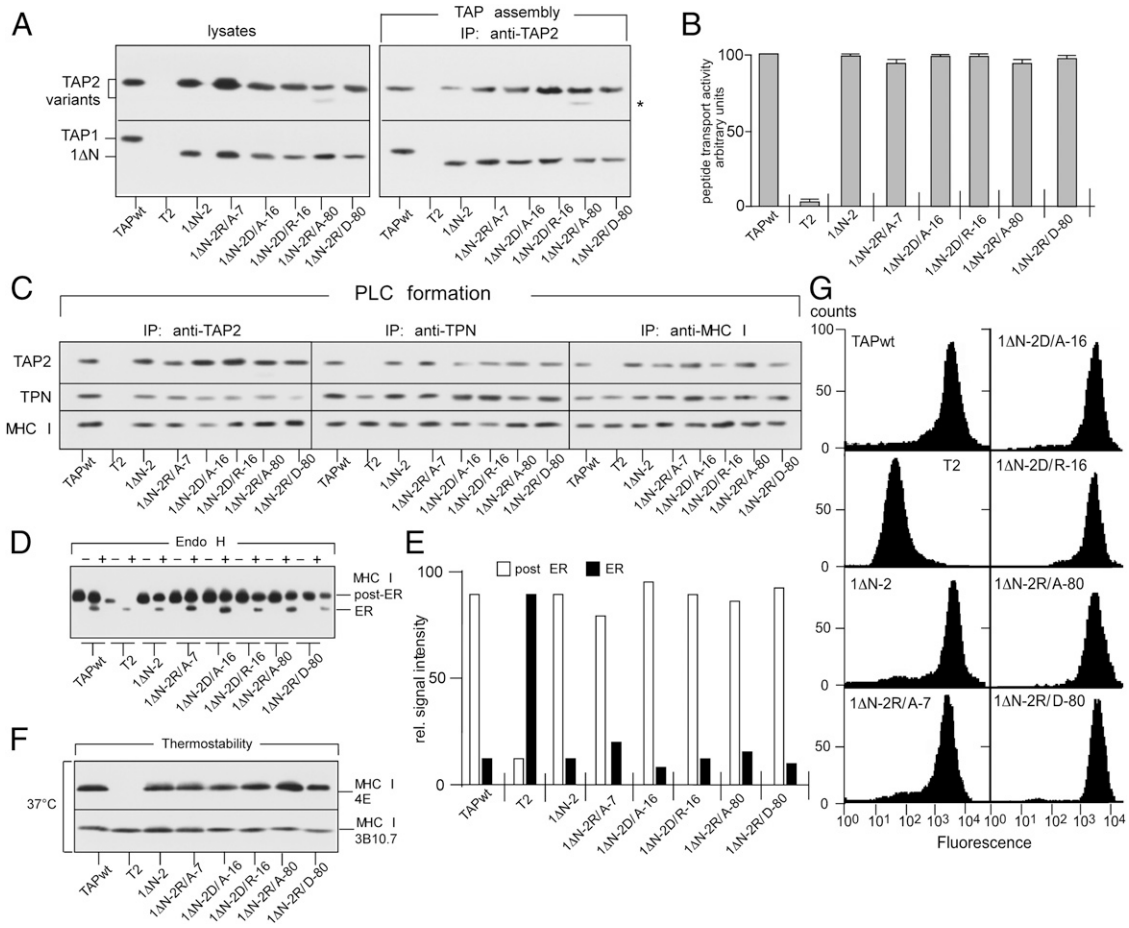

FIGURE 4. Highly conserved acidic and basic residues within and/or adjacent to TM1 and TM2 are dispensable for proper transporter function and the recruitment of TPN/MHC I. (**A**) T2 transfectants expressing TAPwt or the TAP variants 1ΔN-2, 1ΔN-2R/A-7, 1ΔN-2D/A-16, 1ΔN-2D/R-16, 1ΔN-2R/A-80, and 1ΔN-2R/D-80 were lysed in digitonin buffer and subjected to immunoprecipitation using the anti-TAP2 antiserum 116.5. Lysate controls and immunoprecipitates were analyzed by Western blotting. (**B**) Transport activity of wt and mutant TAP variants was measured by a colorimetric assay as described in *Materials and Methods*. The bar graphs represent the average values of experiments carried out in duplicate. (**C**) T2 transfectants were lysed in digitonin, immunoprecipitated with anti-TAP2 (*lanes 1–8*), anti-TPN (*lanes 9–16*), or anti–MHC I (*lanes 17–24*), and analyzed by Western blotting. (**D**) Intracellular maturation of MHC I was assessed by incubating cell lysates with endoglycosidase H (Endo H) followed by Western blotting using the mAb 3B10. Signal quantification was performed by densitometry (**E**). (**F**) Cell lysates of the T2 transfectants were incubated for 1 h at 32°C. The thermostability of HLA-B5 was analyzed by immunoprecipitation using the conformation-dependent and -independent mAbs 4E and 3B10.7. Precipitates were analyzed by Western blotting using mAb 3B10.7. (**G**) Cells were incubated with mAb 4E followed by FITC-labeled secondary Ab. Surface expression of MHC I was determined by flow cytometry. Histograms show life-gated cells.

between the mutant TAP2 variants and TPN, cell lysates of the transiently transfected T2 cells were used for anti-TAP2 immunoprecipitation experiments (Fig. 8B), for immunodepletion studies using TPN-specific Abs (Fig. 8C), as well as for TAP2 stability assays (Fig. 8D). As shown in Fig. 8B, all three TAP2 mutants co-isolated less TPN per immunoprecipitated TAP2 when compared with TAP2wt (i.e., the TAP2/TPN ratio increased from 1.0 to values of 1.3–1.5). This suggests that the central TM leucine residues L20 (TM1) and L66 (TM2) are indeed relevant for proper stoichiometric complex formation between TAP2 and TPN (7, 15). Although the observed TPN-binding differences between wt and TAP2 mutants are small, we could replicate this interesting result by performing quantitative immunodepletion experiments (Fig. 8C). Analysis of TPN-depleted cell extracts demonstrated that a quantitative removal of TPN is normally accompanied by complete codepletion of the transiently transfected TAP2wt. However, this was not observed for TAP2 L/A-20, TAP2 L/A-66, and TAP2 L/A-20:66, although they all displayed a much lower expression level than did TAP2wt (Fig. 8A). For all transfectants expressing mutant TAP2 chains, we again found small but well detectable amounts of TPN-free TAP2 molecules. For instance, T2 transfectants expressing TAP2 L/A-20:66 displayed ~20–22% "TPN-free" TAP2 chains. Moreover, in line with the postulated TAP2 stabilization function of TPN (37), we also found that the half-lives of the three TAP2 mutants were reduced when compared with the half-life of TAP2wt (Fig. 8D). Taken together, our results support the idea that leucine residues within the TMLZs of the first two TMs of TAP2 are part of the hydrophobic interface that is involved in the TPN interaction.

Discussion

Although both N-domains of TAP independently contribute to MHC I/TPN binding, various studies have provided strong evidence for a functional asymmetry with greater significance of the TAP2/TPN interaction for PLC function (7, 15). In line with this, only one TPN bound to TAP2 is sufficient for functional PLC assembly, efficient quality control, and stable peptide loading (7). In the present study, we investigated the biochemical requirements of TAP2/TPN complex formation by employing different transporter variants as PLC model systems. We demonstrate that

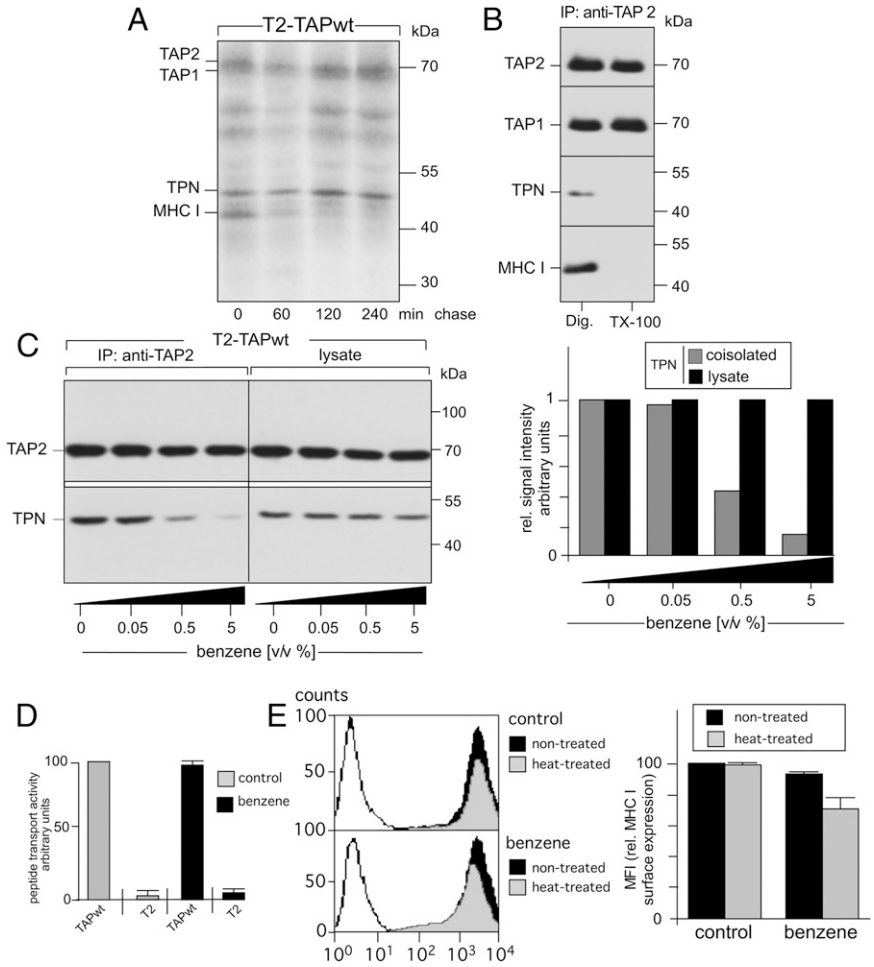

FIGURE 5. Biochemical properties of TAP/TPN interaction. (**A**) Cells were metabolically labeled with [^{35}S]methionine and chased as indicated, before TAP-associated complexes were immunoisolated from digitonin lysates. For a better identification of TAP-associated MHC I molecules, immunoprecipitates were treated with *N*-glycosidase F before SDS-PAGE. (**B**) Digitonin (Dig) or Triton X-100 (TX-100) lysates were immunoprecipitated with TAP-specific Abs and analyzed by Western blotting. (**C**) Digitonin lysates (1% digitonin/1% dioxan in PBS) of T2-TAPwt cells were treated with 0, 0.05, 0.5, or 5% benzene and subjected to immunoprecipitation using anti-TAP2 (116.5). Precipitates and corresponding lysate controls were analyzed by Western blotting (*left panel*). Signal quantification was performed by densitometry (*right panel*). (**D**) To study possible effects of benzene on TAP function, we analyzed the transport activity of TAPwt from T2 transfectants treated or not with 0.1% benzene by a colorimetric assay as described in *Materials and Methods*. The bar graphs represent the average values of experiments carried out in duplicate. Nontransfected TAP$^-$ T2 cells were used as control cells. (**E**) To investigate heat sensitivity of surface HLA-B5, T2 transfectants (expressing TAPwt) treated or not with 0.1% benzene for 24 h were incubated for 10 min at 50°C. Afterward, cells were immunostained with mAb 4E and analyzed by flow cytometry (*left panel*). Flow cytometry results from three independent experiments are presented as the percentage of the mean fluorescence intensities (MFI) of heat-treated cells compared with the MFI of nontreated cells. The MFI (rel. MHC I) of nontreated control cells was set to 100% (*right panel*).

complex formation between TAP2 and TPN is mainly based on hydrophobic interactions between the first two N-terminal TMs of TAP2 and the TM of TPN. Our data show, to our knowledge for the first time, that the hydrocarbon benzene, which interferes with the formation of leucine zippers (19), specifically disrupts the physical interaction between TAP and TPN.

Benzene is a widely used industrial chemical and one of the most common air pollutants (53). Exposure to benzene can lead to deleterious effects in many biological systems, including immune suppression. It was among the first confirmed carcinogens established by the International Agency for Research on Cancer and has been associated with lymphomas, myelodysplastic syndrome, multiple myeloma, and malignant melanoma (54). Our experiments on PLC integrity provide evidence that benzene might directly affect the MHC I Ag presentation machinery in living cells. In particular, thermostability of surface MHC I appears to be detectably reduced (between 20 and 25%) in the presence of the hydrocarbon. If benzene were to separate TAP and TPN in vivo, a reduced thermostability of MHC I would be expected, as TAP incorporation into the PLC is essential for a proper quality control of peptide loading (7, 51, 55). Thus, part of the carcinogenic effect of benzene might be caused by dysfunctional Ag presentation impairing a proper immune response. In our previous studies we had demonstrated that a post-ER quality control checkpoint (dependent on proprotein convertase 7) can rescue unstable MHC I molecules transported to the cell surface of T2 cells (18). This finding could explain the observation that benzene has a rather small effect on the thermostability of surface-expressed MHC I in vivo (Fig. 5E).

Leucine zippers are widespread in nature and are known to frequently mediate interactions between TM proteins (36, 56). Moreover, theoretical calculations (57) and experiments (58, 59) suggest that hydrophobic interactions are more stabilizing than salt bridges in protein folding and assembly. Our studies show that TPN recruitment does not require the presence of the highly conserved arginine and aspartate residues that are juxtaposed to

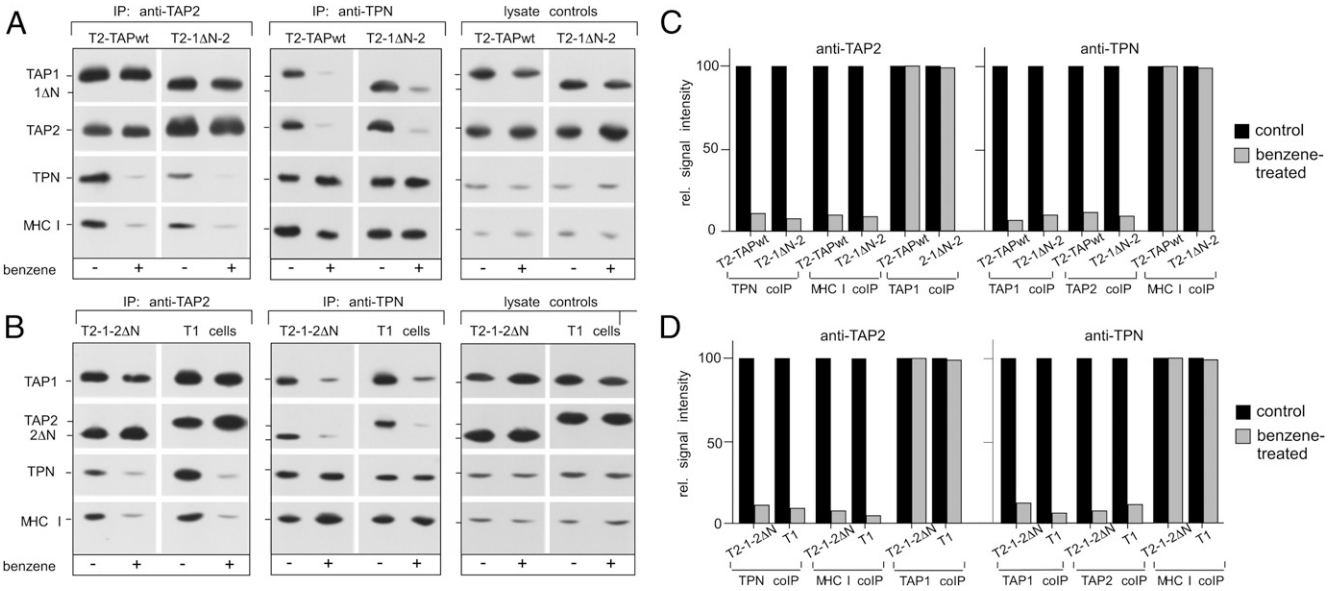

FIGURE 6. TPN/MHC I binding to TAP is specifically disrupted by the hydrophobic effector molecule benzene under PLC-stabilizing conditions. (**A** and **B**) Digitonin lysates (1% digitonin/1% dioxan in PBS) of T2-TAPwt, T2-1ΔN-2, T2-1-2ΔN, and T1 cells were treated or not with 5% benzene and subjected to immunoprecipitation using anti-TAP2 (435.3 and MAC394) (*left panel*) or anti-TPN (PasTa-1) Abs (*middle panel*). Precipitates and corresponding lysate controls (*right panel*) were analyzed by Western blotting. Signal quantification was performed by densitometry. Results are shown in the histograms depicted in (**C**) and (**D**).

the TMLZ motifs of the TM1 and TM2 of TAP2. This is in agreement with a report by Papadopoulos and Momburg (37), who based on an extensive mutational analysis of murine TPN proposed that the TAP2 interaction motif of TPN consists of a TMLZ within the TMD. Most interestingly, a conserved lysine at position 408 within the TMD of TPN (9, 37, 60) does not seem to be required for TAP2/TPN interaction and/or TAP2 stabilization. However, mutations of K408 do cause a failure to stabilize heterodimeric TAP and, as a consequence, abrogate stable PLC formation (61). A possible explanation is that K408 of TPN is required for the transient interaction with the core TMD (not the N-domain) of TAP1 during the biogenesis of functional TAP heterodimers (52). This particular interaction was recently investigated and shown to require polar residues, and is thus probably very different in nature than the TPN association with the TAP N-domains examined in the present study (52). A scenario in which TPN binding to the N-domains and to the core TMD of single TAP1 has different biochemical requirements is further supported by their differential sensitivity to benzene (Figs. 5, 6, Supplemental Fig. 1). The interactions are likely also functionally different, as binding the core TMD of TAP1 occurs only very transiently during transporter assembly, whereas TAP forms a stable, permanent unit with TPN via its N-domains (12). Hence, it seems that TPN uses distinct mechanisms, as the molecule associates with various regions within TAP during the biogenesis of the PLC.

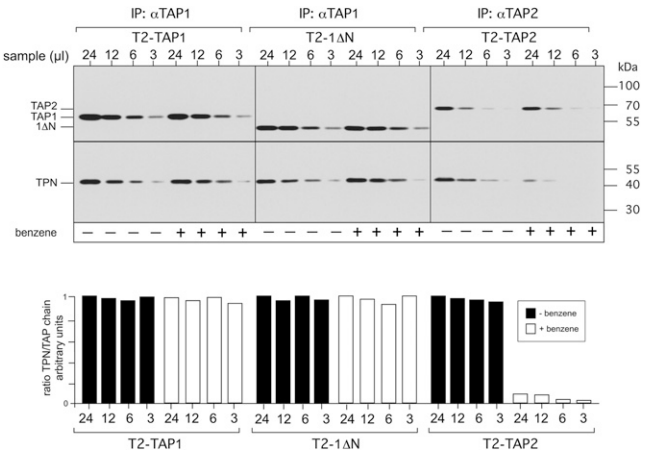

FIGURE 7. TPN interactions of single TAP1 and TAP2 chains differ in their benzene sensitivity. Digitonin lysates of T2-TAP1, T2-1ΔN, and T2-TAP2 cells were treated or not with 5% benzene and subjected to immunoprecipitation using protein A–Sepharose-coupled anti-TAP1 (D90) and anti-TAP2 (116.5) Abs. Precipitates of different sample volumes (24, 12, 6, and 3 μl) were analyzed by Western blotting using Abs against TAP1, TAP2, and TPN. Signal quantification was performed by densitometry. Histograms showing the obtained TPN/TAP chain signal ratio are depicted below the respective immunoblots.

Our results suggest that the TM1 and TM2 of TAP2 cooperate in recruiting TPN. Thus, the TMLZs of the TAP2-TM1, the TAP2-TM2, and the TPN-TM may form a trimeric unit, as has been described for other membrane-bound protein complexes (36). Thus, for example, the chicken homolog of the hepatic asialoglycoprotein receptors exists as a homotrimer whose formation and stability depend on the TMLZ sequences (62, 63). Moreover, heteromeric cyclic nucleotide-gated channels require for their stable assembly trimer-forming C-terminal leucine zippers (64). Furthermore, also several viral proteins exist as oligomeric complexes, and their assembly appears to depend on the TMLZ within their TMs. For instance, the influenza hemagglutinin TM with its leucine-rich sequence motifs is required for full membrane fusion (65) and stabilizes the trimeric complex (66). Moreover, mutations of conserved leucine residues within the TMs of the hemagglutinin-neuraminidase of Newcastle disease virus affect tetramerization and fusion promotion (67).

Thus, such an arrangement within the PLC might explain the high specificity as well as structural stability of TAP/TPN complexes. TM α helices that are used for the assembly of TM proteins can have the same or opposite orientations within membranes (56, 68, 69). Thus, one can imagine that in the TAP2/TPN complex the antiparallel TM1/TM2 orientation in TAP2 forms a hydrophobic

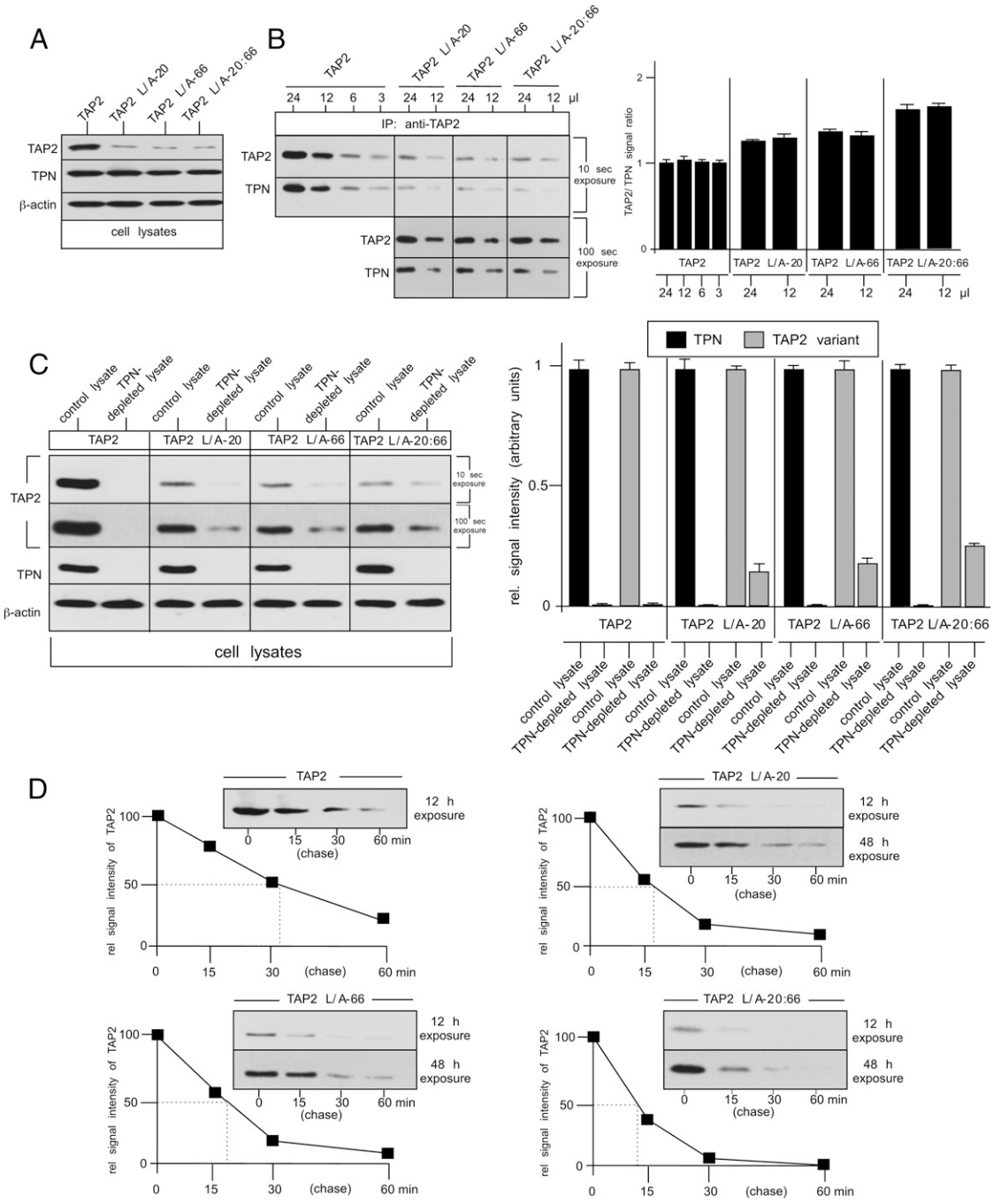

FIGURE 8. Functional role of leucine residues in the TMLZ of TAP2. (**A** and **B**) Immunoisolation of TAP2/TPN complexes. Digitonin lysates of transiently transfected T2-TAP2, T2-TAP2 L/A-20, T2-TAP2 L/A-66, and T2-TAP2 L/A-20:66 cells (A) were subjected to immunoprecipitation using anti-TAP2 (B). Precipitates of different sample volume (from 24 to 3 μl) were analyzed by Western blotting using Abs against TAP2 and TPN. One representative result (with two different exposures [10 and 100 s] of the mutant TAP2 blots) of three independent experiments is shown (*left*). Signal quantification was performed by densitometry. Data of all experiments are summarized in the histogram plot showing the obtained TAP2/TPN signal ratios (*right*). (**C**) Immunodepletion of TAP2/TPN complexes. Digitonin lysates of transiently transfected T2-TAP2, T2-TAP2 L/A-20, T2-TAP2 L/A-66, and T2-TAP2 L/A-20:66 cells were incubated with either control Sepharose (mock-depleted control lysate treated with an irrelevant mouse IgG Ab coupled to cyanogen bromide [CNBr]–activated Sepharose) or subjected to quantitative immunodepletion of TPN/TAP2 complexes using CNBr-Sepharose–conjugated anti-TPN (anti-TPN treated lysates). All cell lysates were analyzed in Western blots probed for TAP2, TPN, and β-actin of the TAP2 blots. One representative result (with two different exposures of the TAP2 blots [10 and 100 s]) of three independent experiments is shown (*left*). Signal quantification was performed by densitometry. Data of all experiments are summarized in the histogram plot showing the obtained signals of TPN and TAP2 in the mock-depleted control lysates and the TPN-depleted lysates (*right*). (**D**) In vivo stability of different TAP2 variants. Twenty-four hours after nucleofection the T2 transfectants expressing the different TAP2 variants were biosynthetically labeled for 30 min and chased for 0, 15, 30, and 60 min. Lysates were immunoprecipitated with anti-TAP2 and resolved on a 10% SDS gel. Quantification was performed by densitometric analysis of the corresponding autoradiographs. For the mutant TAP2 chains, autoradiographs with two different exposures (12 and 48 h) are shown. The depicted plots show the percentage of precipitated radiolabeled TAP2 at each time point relative to the amount of TAP chains isolated directly after the pulse.

core, against which the TM of TPN is packed. Indeed, the TM of TPN and each of the two N-terminal TMs of TAP2 contain broad hydrophobic leucine-rich surface areas (see Fig. 1), which may allow the assembly of a hydrophobic three-stranded α helix unit. Note that the valine-rich TM segments of the MHC I (HLA-B51, GenBank accession no. AAA64513.1, TM segment, IVAGLAVLAVVVI-GAVVAAVMC; HLA-A2, GenBank accession no. AAA76608.2, TM segment, GIIAGLVLFGAVITGAVVAAVMW) expressed in T2 cells apparently do not contain TMLZs. Thus, it is rather unlikely that TM segments of MHC I play any role in the TMLZ-mediated complex formation between TAP and TPN. This is in line with the hypothesis that TPN and MHC I interact with each other via their ER luminal domains (70). The TMLZs of TM1 and TM2 are present in both TAP chains at corresponding sequence positions. Fig. 9 shows a hypothetical working model in which we propose that the TM segment of TPN may be able to interact via two pairing leucine zipper–like structures with respective hydrophobic motives in TM1 (containing the TMLZ with L20) and TM2 (containing the TMLZ with L66) of both TAP chains. In our model, which does not contain any salt bridges, the composition of the involved leucine zipper–like structures may be somewhat different between TAP1 and TAP2, and the TMLZs of TAP2 seem to represent more ideal leucine zipper motifs than do the TMLZs of TAP1. This could be one of the possible factors contributing to the observed functional asymmetry of the two TPN-docking sites of TAP1 and TAP2 (7, 15). Similar to the first TM of TAP2, also the TM1 of TAP1 contains a highly conserved aspartate (D17, Fig. 1) at homologous sequence position (e.g., D16-rat TAP2, D17-rat TAP1). Based on our work, it is tempting to speculate that in the case of TAP1 this acidic residue in the N-domain may be also dispensable for the functional TAP1/TPN interaction. Mutations of the conserved aspartate in TAP2 seem to have no effect on TPN interaction and peptide transport function of TAP (see Fig. 4). However, unfortunately, TAP mutants carrying aspartate mutations in the TM1 of TAP1 are characterized by very low steady-state expression of the TAP1 chains (data not shown). Thus, it has so far not been possible to directly compare the function of the conserved aspartate in the TM1 of TAP1 and TAP2. The three conserved charged basic residues in the TM1/TM2 sequence of TAP1 are arginines at positions R22, R40, and R48, which have apparently no respective counterpart residues in the TM1/TM2 sequence of TAP2 (Fig. 1). Reciprocally, the same is also true for the conserved basic TM1/TM2 residues of TAP2. These sequence differences probably do not play a role for the differential effect of benzene on the single–chain TAP1/TPN and single-chain TAP2/TPN interaction because unassembled TAP1 uses its core domain and not the N-domain for the binding to TPN. However, it will be highly interesting to see whether and to what extent these sequence differences are responsible for the observed dissimilar properties of the two MHC I loading sites in the PLC (7, 15). Clearly, more work is required to find out whether and to what extent sequence differences in the N-terminal TMs are responsible for the observed functional differences in TPN recruitment between TAP1 and TAP2.

Our findings do not support the original view that merely the first N-terminal TM of each N-domain is involved in TPN recruitment (8). Because TPN binding by TAP is structurally conserved among distinct vertebrates (14), species–specific differences are very unlikely to account for the different results of the studies. We suggest that the discrepancy is most likely due to the fact that Koch et al. (8) used a baculovirus/insect cell expression system, which is known to generate large amount of proteolyzed TAP variants that are deprived of their N-domain sequences essentially required for TPN binding (11). Another critical experimental limit of the baculovirus system is that important accessory interactions between the different components of the PLC are missing. In vertebrates, TPN normally binds via a covalent bond to ERp57, which interacts with calreticulin, which in turn associates with MHC I forming a complex with TPN (10, 71). All of these interactions individually contribute only little to the overall stability of the PLC, but in sum they enormously stabilize the complex (10). Because insect cells do not express MHC I molecules, crucial interactions in the artificially formed PLC are absent. Fur-

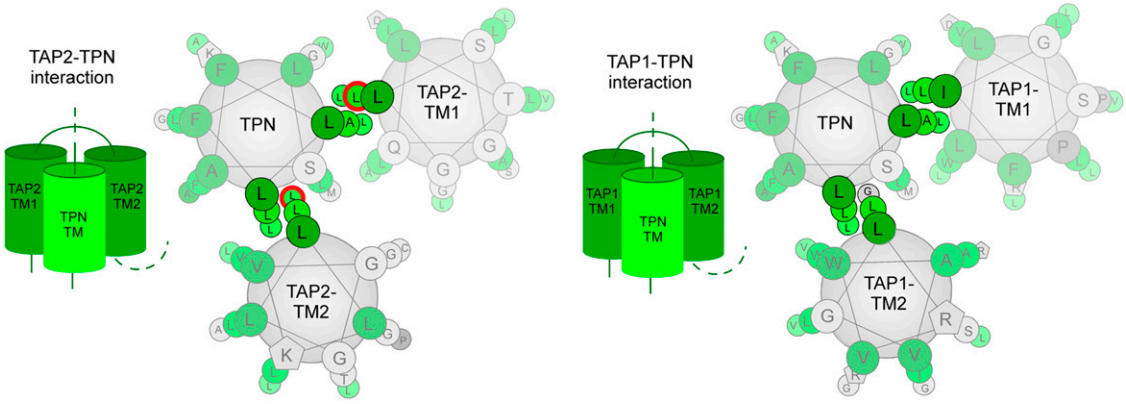

FIGURE 9. Hypothetical working model on the possible TM interactions between TPN and TAP1 and TAP2. Topology prediction of the TMDs was performed with TopPred II (see Fig. 1). Using a modeling related to the style of the online prediction tool DrawCoil 1.0 (http://www.grigoryanlab.org/drawcoil/) single helical wheels were generated for the TM segment of TPN (37) and each of the first two TMs of TAP1 and TAP2 and then spatially arranged for the hypothetical TM interaction model. For a simple graphical representation, the residues, which emanate from the same angular position of the helices (at the seventh heptad repeat position), are row arranged in the different helical wheel diagrams. For this kind of modeling we used the respective consensus sequences of TPN, TAP1, and TAP2 from humans, mice, and rats. The postulated membrane orientations of TM1 and TM2 in the proposed model are based on findings that were currently published by Hulpke et al. (12, 15). Because our study did not analyze structural interactions between the N-terminal TMs of TAP1 and TAP2, the depicted working model does not speculate on (or consider) possible contacts/interfaces between TM1 and TM2 of the two TAP chains. The leucine zippers and hydrophobic residues in the helical wheel projections of TPN, TAP1-TM1/TM2, and TAP2-TM1/TM2 are shown in green. Leucine residues that could be exchanged to alanine by site-directed mutagenesis in TM1 and TM2 of TAP2 (L-20 and L66) are marked by a red circles. All TAP and TPN sequences used for the hypothetical working model were retrieved from the GenBank database (http://www.ncbi.nlm.nih.gov/genbank/) (GenBank accession nos. AJ400732.1, AJ316613.2, AF009510.1, X63854.1, NM_011530.3, AB073779.1, X57523.1, NM_001161730.1, and AY523971.2).

thermore, it is not clear whether oxidoreductases and chaperones from insect cells can functionally substitute for the auxiliary PLC components ERp57 and calreticulin. Thus, partially assembled PLC variants formed in baculovirus-infected invertebrate cells (8) are likely to be unstable and may fall apart during immunoisolation. Fragile complexes held together by residual weak interactions could easily go undetected.

The greater resistance of TAP1/TAP2 and TPN/MHC interactions to the effects of benzene might be also due to the fact that TAP1/TAP2 complexes are predicted to involve multiple interdigitating TM domain interactions and that TPN/MHC interactions involve the luminal domains of the proteins. However, these two explanations clearly do not work for the observed benzene resistance of TAP1/TPN and 1ΔN/TPN complexes. Previous studies have demonstrated that in the case of single unassembled TAP1 chains a polar face of TM9 in the core TMD is essential to establish an interaction with TPN during the proper heterodimerization of the transporter (52). Our present findings (Fig. 7) clearly show that this TPN recruitment to the polar TM helix of single TAP1 is much more resistant to benzene than is the TPN binding to the two leucine-rich N-terminal TMs of TAP1 and TAP2. Unlike the TM1 and TM2 of both TAP chains, the TM9 of TAP1 does not contain a TMLZ motif. Thus, it is tempting to speculate that the observed differential effects of benzene on TPN interaction rely predominantly on the hydrophobic and/or polar character of the respective interface and are therefore rather specific to the N-terminal TMs of TAP.

Which molecular factors may contribute to the specificity of the hydrophobic TAP2/TPN interaction? There are several cases in which interactions between TM α helices are highly specific in the absence of prosthetic groups (72). Examples include the dimerization of the single TM α helix of human glycophorin A (73–75) and the association of the TMDs of the MHC II α- and β-chains (76). In these cases, a precise pattern of hydrophobic amino acid side chains on one face of the TM α helix is required for helix/helix interactions. Various studies have shown that van der Waals interactions alone can provide sufficiently stabilizing forces to mediate specific TM α helix associations (77–79). A similar hydrophobic mechanism may drive the specific assembly of the TM α helices of TAP and TPN.

The adenovirus TM protein E3-19K delays the surface expression of MHC I alleles to which it cannot bind tightly (80). It was proposed that E3-19K mimics the TAP-binding site on TPN, allowing it to function as a specific competitive inhibitor (81). This would imply a certain structural relatedness between E3-19K and TPN at the level of their TMDs. Interestingly, the TM of E3-19K is characterized by a leucine-rich sequence stretch that does not comprise any charged basic and/or acidic residues suitable for salt bridge formation (82). Because E3-19K attacks the TPN-docking site of TAP1 and TAP2 via its TM region (81), complex formation may be based on hydrophobic protein interactions as well.

TAP variants lacking the N-domain of TAP2 (e.g., 1-2ΔN) (7) display altered PLC formation properties with reduced complex stability as well as quality control in MHC I loading (7, 83). This makes it very difficult to determine the structural requirements of the N-domain of TAP1 for TPN interaction as it was performed for the N-domain of TAP2 in the present study. Nevertheless, the benzene sensitivity of the TPN interaction of TAPwt (in T1 and T2 cells) and variant 1-2ΔN (in T2 transfectants) as well as the presence of highly conserved leucine-rich hydrophobic sequence stretches within the first two N-terminal TMs of TAP1 (see Fig. 1) strongly suggest that also in this case complex formation is mainly based on hydrophobic interactions. In line with this, it was demonstrated by others (51) that mutations of a conserved leucine residue in the TMLZ of TPN profoundly affect the interaction with and stabilization of TAP1.

In conclusion, our study provides strong evidence that hydrophobic interactions drive TAP/TPN complex formation and it offers a new angle on N-domain function in TPN recruitment and PLC formation.

Acknowledgments

We are grateful to Peter Cresswell for supplying anti-TPN Abs. We thank Markus Kreutzer for excellent technical assistance and Lothar Stitz for critically reading and commenting on the manuscript. We thank the reviewers for constructive remarks on the paper, as these comments led us to an improvement of the work.

Disclosures

The authors have no financial conflicts of interest.

References

1. Dimberu, P. M., and R. M. Leonhardt. 2011. Cancer immunotherapy takes a multi-faceted approach to kick the immune system into gear. *Yale J. Biol. Med.* 84: 371–380.
2. Gaczynska, M., K. L. Rock, and A. L. Goldberg. 1993. Role of proteasomes in antigen presentation. *Enzyme Protein* 47: 354–369.
3. Rufer, E., R. M. Leonhardt, and M. R. Knittler. 2007. Molecular architecture of the TAP-associated MHC class I peptide-loading complex. *J. Immunol.* 179: 5717–5727.
4. Beismann-Driemeyer, S., and R. Tampé. 2004. Function of the antigen transport complex TAP in cellular immunity. *Angew. Chem. Int. Ed. Engl.* 43: 4014–4031.
5. Pamer, E., and P. Cresswell. 1998. Mechanisms of MHC class I—restricted antigen processing. *Annu. Rev. Immunol.* 16: 323–358.
6. Alberts, P., O. Daumke, E. V. Deverson, J. C. Howard, and M. R. Knittler. 2001. Distinct functional properties of the TAP subunits coordinate the nucleotide-dependent transport cycle. *Curr. Biol.* 11: 242–251.
7. Leonhardt, R. M., K. Keusekotten, C. Bekpen, and M. R. Knittler. 2005. Critical role for the tapasin-docking site of TAP2 in the functional integrity of the MHC class I-peptide-loading complex. *J. Immunol.* 175: 5104–5114.
8. Koch, J., R. Guntrum, S. Heintke, C. Kyritsis, and R. Tampé. 2004. Functional dissection of the transmembrane domains of the transporter associated with antigen processing (TAP). *J. Biol. Chem.* 279: 10142–10147.
9. Ortmann, B., J. Copeman, P. J. Lehner, B. Sadasivan, J. A. Herberg, A. G. Grandea, S. R. Riddell, R. Tampé, T. Spies, J. Trowsdale, and P. Cresswell. 1997. A critical role for tapasin in the assembly and function of multimeric MHC class I-TAP complexes. *Science* 277: 1306–1309.
10. Wearsch, P. A., and P. Cresswell. 2008. The quality control of MHC class I peptide loading. *Curr. Opin. Cell Biol.* 20: 624–631.
11. Procko, E., G. Raghuraman, D. C. Wiley, M. Raghavan, and R. Gaudet. 2005. Identification of domain boundaries within the N-termini of TAP1 and TAP2 and their importance in tapasin binding and tapasin-mediated increase in peptide loading of MHC class I. *Immunol. Cell Biol.* 83: 475–482.
12. Hulpke, S., C. Baldauf, and R. Tampé. 2012. Molecular architecture of the MHC I peptide-loading complex: one tapasin molecule is essential and sufficient for antigen processing. *FASEB J.* 26: 5071–5080.
13. Panter, M. S., A. Jain, R. M. Leonhardt, T. Ha, and P. Cresswell. 2012. Dynamics of major histocompatibility complex class I association with the human peptide-loading complex. *J. Biol. Chem.* 287: 31172–31184.
14. Hinz, A., J. Jedamzick, V. Herbring, H. Fischbach, J. Hartmann, D. Parcej, J. Koch, and R. Tampé. 2014. Assembly and function of the major histocompatibility complex (MHC) I peptide-loading complex are conserved across higher vertebrates. *J. Biol. Chem.* 289: 33109–33117.
15. Hulpke, S., M. Tomioka, E. Kremmer, K. Ueda, R. Abele, and R. Tampé. 2012. Direct evidence that the N-terminal extensions of the TAP complex act as autonomous interaction scaffolds for the assembly of the MHC I peptide-loading complex. *Cell. Mol. Life Sci.* 69: 3317–3327.
16. Walker, B. A., A. van Hateren, S. Milne, S. Beck, and J. Kaufman. 2005. Chicken TAP genes differ from their human orthologues in locus organisation, size, sequence features and polymorphism. *Immunogenetics* 57: 232–247.
17. Kaufman, J. 2013. Antigen processing and presentation: evolution from a bird's eye view. *Mol. Immunol.* 55: 159–161.
18. Leonhardt, R. M., D. Fiegl, E. Rufer, A. Karger, B. Bettin, and M. R. Knittler. 2010. Post-endoplasmic reticulum rescue of unstable MHC class I requires proprotein convertase PC7. *J. Immunol.* 184: 2985–2998.
19. Gonzalez, L., Jr., J. J. Plecs, and T. Alber. 1996. An engineered allosteric switch in leucine-zipper oligomerization. *Nat. Struct. Biol.* 3: 510–515.
20. Yadav, M. K., J. E. Redman, L. J. Leman, J. M. Alvarez-Gutiérrez, Y. Zhang, C. D. Stout, and M. R. Ghadiri. 2005. Structure-based engineering of internal cavities in coiled-coil peptides. *Biochemistry* 44: 9723–9732.
21. DeMars, R., C. C. Chang, S. Shaw, P. J. Reitnauer, and P. M. Sondel. 1984. Homozygous deletions that simultaneously eliminate expressions of class I and class II antigens of EBV-transformed B-lymphoblastoid cells. I. Reduced proliferative responses of autologous and allogeneic T cells to mutant cells that have decreased expression of class II antigens. *Hum. Immunol.* 11: 77–97.
22. Salter, R. D., D. N. Howell, and P. Cresswell. 1985. Genes regulating HLA class I antigen expression in T-B lymphoblast hybrids. *Immunogenetics* 21: 235–246.

23. Schwartz, D. P., C. R. Brewington, and L. H. Burgwald. 1967. Rapid quantitative procedure for removing cholesterol from butter fat. *J. Lipid Res.* 8: 54–55.
24. Gunning, P., J. Leavitt, G. Muscat, S. Y. Ng, and L. Kedes. 1987. A human beta-actin expression vector system directs high-level accumulation of antisense transcripts. *Proc. Natl. Acad. Sci. USA* 84: 4831–4835.
25. Momburg, F., V. Ortiz-Navarrete, J. Neefjes, E. Goulmy, Y. van de Wal, H. Spits, S. J. Powis, G. W. Butcher, J. C. Howard, P. Walden, et al. 1992. Proteasome subunits encoded by the major histocompatibility complex are not essential for antigen presentation. *Nature* 360: 174–177.
26. Powis, S. J., A. R. Townsend, E. V. Deverson, J. Bastin, G. W. Butcher, and J. C. Howard. 1991. Restoration of antigen presentation to the mutant cell line RMA-S by an MHC-linked transporter. *Nature* 354: 528–531.
27. Knittler, M. R., K. Gülow, A. Seelig, and J. C. Howard. 1998. MHC class I molecules compete in the endoplasmic reticulum for access to transporter associated with antigen processing. *J. Immunol.* 161: 5967–5977.
28. Meyer, T. H., P. M. van Endert, S. Uebel, B. Ehring, and R. Tampé. 1994. Functional expression and purification of the ABC transporter complex associated with antigen processing (TAP) in insect cells. *FEBS Lett.* 351: 443–447.
29. van Endert, P. M., R. Tampé, T. H. Meyer, R. Tisch, J. F. Bach, and H. O. McDevitt. 1994. A sequential model for peptide binding and transport by the transporters associated with antigen processing. *Immunity* 1: 491–500.
30. Lutz, P. M., and P. Cresswell. 1987. An epitope common to HLA class I and class II antigens, Ig light chains, and β_2-microglobulin. *Immunogenetics* 25: 228–233.
31. Dick, T. P., N. Bangia, D. R. Peaper, and P. Cresswell. 2002. Disulfide bond isomerization and the assembly of MHC class I-peptide complexes. *Immunity* 16: 87–98.
32. Schägger, H., W. A. Cramer, and G. von Jagow. 1994. Analysis of molecular masses and oligomeric states of protein complexes by blue native electrophoresis and isolation of membrane protein complexes by two-dimensional native electrophoresis. *Anal. Biochem.* 217: 220–230.
33. Ehses, S., R. M. Leonhardt, G. Hansen, and M. R. Knittler. 2005. Functional role of C-terminal sequence elements in the transporter associated with antigen processing. *J. Immunol.* 174: 328–339.
34. Keusekotten, K., R. M. Leonhardt, S. Ehses, and M. R. Knittler. 2006. Biogenesis of functional antigenic peptide transporter TAP requires assembly of pre-existing TAP1 with newly synthesized TAP2. *J. Biol. Chem.* 281: 17545–17551.
35. Claros, M. G., and G. von Heijne. 1994. TopPred II: an improved software for membrane protein structure predictions. *Comput. Appl. Biosci.* 10: 685–686.
36. Gurezka, R., R. Laage, B. Brosig, and D. Langosch. 1999. A heptad motif of leucine residues found in membrane proteins can drive self-assembly of artificial transmembrane segments. *J. Biol. Chem.* 274: 9265–9270.
37. Papadopoulos, M., and F. Momburg. 2007. Multiple residues in the transmembrane helix and connecting peptide of mouse tapasin stabilize the transporter associated with the antigen-processing TAP2 subunit. *J. Biol. Chem.* 282: 9401–9410.
38. Gao, B., A. Williams, A. Sewell, and T. Elliott. 2004. Generation of a functional, soluble tapasin protein from an alternatively spliced mRNA. *Genes Immun.* 5: 101–108.
39. Walther, T. H., and A. S. Ulrich. 2014. Transmembrane helix assembly and the role of salt bridges. *Curr. Opin. Struct. Biol.* 27: 63–68.
40. Cohen, C., and D. A. Parry. 1990. α-Helical coiled coils and bundles: how to design an α-helical protein. *Proteins* 7: 1–15.
41. Phelan, P., A. A. Gorfe, I. Jelesarov, D. N. Marti, J. Warwicker, and H. R. Bosshard. 2002. Salt bridges destabilize a leucine zipper designed for maximized ion pairing between helices. *Biochemistry* 41: 2998–3008.
42. Diedrich, G., N. Bangia, M. Pan, and P. Cresswell. 2001. A role for calnexin in the assembly of the MHC class I loading complex in the endoplasmic reticulum. *J. Immunol.* 166: 1703–1709.
43. Li, S., H. O. Sjögren, U. Hellman, R. F. Pettersson, and P. Wang. 1997. Cloning and functional characterization of a subunit of the transporter associated with antigen processing. *Proc. Natl. Acad. Sci. USA* 94: 8708–8713.
44. Peaper, D. R., and P. Cresswell. 2008. The redox activity of ERp57 is not essential for its functions in MHC class I peptide loading. *Proc. Natl. Acad. Sci. USA* 105: 10477–10482.
45. Sikkema, J., J. A. de Bont, and B. Poolman. 1995. Mechanisms of membrane toxicity of hydrocarbons. *Microbiol. Rev.* 59: 201–222.
46. Papaloukas, C., E. Granseth, H. Viklund, and A. Elofsson. 2008. Estimating the length of transmembrane helices using Z-coordinate predictions. *Protein Sci.* 17: 271–278.
47. Porte, D., P. Oertel-Buchheit, M. Granger-Schnarr, and M. Schnarr. 1995. Fos leucine zipper variants with increased association capacity. *J. Biol. Chem.* 270: 22721–22730.
48. Guy, H. R., and G. Raghunathan. 1988. Structural models for membrane insertion and channel formation by antiparallel alpha helical membrane peptides. *Jerusalem Symp. Quantum Chem. Biochem.* 21: 369–379.
49. Portenhauser, R., and O. Wieland. 1972. Regulation of pyruvate dehydrogenase in mitochondria of rat liver. *Eur. J. Biochem.* 31: 308–314.
50. Dees, C., T. L. German, W. F. Wade, and R. F. Marsh. 1985. Characterization of lipids in membrane vesicles from scrapie-infected hamster brain. *J. Gen. Virol.* 66: 861–870.
51. Tan, P., H. Kropshofer, O. Mandelboim, N. Bulbuc, G. J. Hämmerling, and F. Momburg. 2002. Recruitment of MHC class I molecules by tapasin into the transporter associated with antigen processing-associated complex is essential for optimal peptide loading. *J. Immunol.* 168: 1950–1960.
52. Leonhardt, R. M., P. Abrahimi, S. M. Mitchell, and P. Cresswell. 2014. Three tapasin docking sites in TAP cooperate to facilitate transporter stabilization and heterodimerization. *J. Immunol.* 192: 2480–2494.
53. Sonawane, B., D. Bayliss, L. Valcovic, C. Chen, B. Rodan, and W. Farland, Environmental Protection Agency. 2000. Carcinogenic effects of benzene—a status update and research needs to improve risk assessments: US EPA perspective. *J. Toxicol. Environ. Health A* 61: 471–472.
54. International Agency for Research on Cancer. 1987. *IARC Monographs on the Evaluation of Carcinogenic Risks to Humans.*, Suppl. 7. Overall Evaluations of Carcinogenicity: An Updating of IARC Monographs, Vols. 1–42. International Agency for Research on Cancer, Lyon, France, p. 120–121.
55. Williams, A. P., C. A. Peh, A. W. Purcell, J. McCluskey, and T. Elliott. 2002. Optimization of the MHC class I peptide cargo is dependent on tapasin. *Immunity* 16: 509–520.
56. Gurezka, R., and D. Langosch. 2001. In vitro selection of membrane-spanning leucine zipper protein-protein interaction motifs using POSSYCCAT. *J. Biol. Chem.* 276: 45580–45587.
57. Hendsch, Z. S., and B. Tidor. 1994. Do salt bridges stabilize proteins? A continuum electrostatic analysis. *Protein Sci.* 3: 211–226.
58. Waldburger, C. D., J. F. Schildbach, and R. T. Sauer. 1995. Are buried salt bridges important for protein stability and conformational specificity? *Nat. Struct. Biol.* 2: 122–128.
59. Wimley, W. C., K. Gawrisch, T. P. Creamer, and S. H. White. 1996. Direct measurement of salt-bridge solvation energies using a peptide model system: implications for protein stability. *Proc. Natl. Acad. Sci. USA* 93: 2985–2990.
60. Deverson, E. V., S. J. Powis, N. A. Morrice, J. A. Herberg, J. Trowsdale, and G. W. Butcher. 2001. Rat tapasin: cDNA cloning and identification as a component of the class I MHC assembly complex. *Genes Immun.* 2: 48–51.
61. Petersen, J. L., H. D. Hickman-Miller, M. M. McIlhaney, S. E. Vargas, A. W. Purcell, W. H. Hildebrand, and J. C. Solheim. 2005. A charged amino acid residue in the transmembrane/cytoplasmic region of tapasin influences MHC class I assembly and maturation. *J. Immunol.* 174: 962–969.
62. Loeb, J. A., and K. Drickamer. 1987. The chicken receptor for endocytosis of glycoproteins contains a cluster of *N*-acetylglucosamine-binding sites. *J. Biol. Chem.* 262: 3022–3029.
63. Verrey, F., and K. Drickamer. 1993. Determinants of oligomeric structure in the chicken liver glycoprotein receptor. *Biochem. J.* 292: 149–155.
64. Zhong, H., J. Lai, and K. W. Yau. 2003. Selective heteromeric assembly of cyclic nucleotide-gated channels. *Proc. Natl. Acad. Sci. USA* 100: 5509–5513.
65. Kemble, G. W., T. Danieli, and J. M. White. 1994. Lipid-anchored influenza hemagglutinin promotes hemifusion, not complete fusion. *Cell* 76: 383–391.
66. Doms, R. W., and A. Helenius. 1986. Quaternary structure of influenza virus hemagglutinin after acid treatment. *J. Virol.* 60: 833–839.
67. McGinnes, L., T. Sergel, and T. Morrison. 1993. Mutations in the transmembrane domain of the HN protein of Newcastle disease virus affect the structure and activity of the protein. *Virology* 196: 101–110.
68. O'Shea, E. K., J. D. Klemm, P. S. Kim, and T. Alber. 1991. X-ray structure of the GCN4 leucine zipper, a two-stranded, parallel coiled coil. *Science* 254: 539–544.
69. Lu, M., S. C. Blacklow, and P. S. Kim. 1995. A trimeric structural domain of the HIV-1 transmembrane glycoprotein. *Nat. Struct. Biol.* 2: 1075–1082.
70. Turnquist, H. R., S. E. Vargas, E. L. Schenk, M. M. McIlhaney, A. J. Reber, and J. C. Solheim. 2002. The interface between tapasin and MHC class I: identification of amino acid residues in both proteins that influence their interaction. *Immunol. Res.* 25: 261–269.
71. Dong, G., P. A. Wearsch, D. R. Peaper, P. Cresswell, and K. M. Reinisch. 2009. Insights into MHC class I peptide loading from the structure of the tapasin-ERp57 thiol oxidoreductase heterodimer. *Immunity* 30: 21–32.
72. Lemmon, M. A., and D. M. Engelman. 1994. Specificity and promiscuity in membrane helix interactions. *FEBS Lett.* 346: 17–20.
73. Bormann, B. J., W. J. Knowles, and V. T. Marchesi. 1989. Synthetic peptides mimic the assembly of transmembrane glycoproteins. *J. Biol. Chem.* 264: 4033–4037.
74. Lemmon, M. A., J. M. Flanagan, J. F. Hunt, B. D. Adair, B. J. Bormann, C. E. Dempsey, and D. M. Engelman. 1992. Glycophorin A dimerization is driven by specific interactions between transmembrane α-helices. *J. Biol. Chem.* 267: 7683–7689.
75. Lemmon, M. A., J. M. Flanagan, H. R. Treutlein, J. Zhang, and D. M. Engelman. 1992. Sequence specificity in the dimerization of transmembrane α-helices. *Biochemistry* 31: 12719–12725.
76. Cosson, P., and J. S. Bonifacino. 1992. Role of transmembrane domain interactions in the assembly of class II MHC molecules. *Science* 258: 659–662.
77. Adams, P. D., I. T. Arkin, D. M. Engelman, and A. T. Brünger. 1995. Computational searching and mutagenesis suggest a structure for the pentameric transmembrane domain of phospholamban. *Nat. Struct. Biol.* 2: 154–162.
78. Adams, P. D., D. M. Engelman, and A. T. Brünger. 1996. Improved prediction for the structure of the dimeric transmembrane domain of glycophorin A obtained through global searching. *Proteins* 26: 257–261.
79. Fleming, K. G., and D. M. Engelman. 2001. Computation and mutagenesis suggest a right-handed structure for the synaptobrevin transmembrane dimer. *Proteins* 45: 313–317.
80. Bennett, E. M., J. R. Bennink, J. W. Yewdell, and F. M. Brodsky. 1999. Cutting edge: adenovirus E19 has two mechanisms for affecting class I MHC expression. *J. Immunol.* 162: 5049–5052.
81. Hansen, T. H., and M. Bouvier. 2009. MHC class I antigen presentation: learning from viral evasion strategies. *Nat. Rev. Immunol.* 9: 503–513.
82. Flomenberg, P., J. Szmulewicz, E. Gutierrez, and H. Lupatkin. 1992. Role of the adenovirus E3-19k conserved region in binding major histocompatibility complex class I molecules. *J. Virol.* 66: 4778–4783.
83. Verweij, M. C., D. Koppers-Lalic, S. Loch, F. Klauschies, H. de la Salle, E. Quinten, P. J. Lehner, A. Mulder, M. R. Knittler, R. Tampé, et al. 2008. The varicellovirus UL49.5 protein blocks the transporter associated with antigen processing (TAP) by inhibiting essential conformational transitions in the 6+6 transmembrane TAP core complex. *J. Immunol.* 181: 4894–4907.